This copy of the ESI replaces the previous version published on 6th December 2022

Noncovalent wedging effect catalyzed the *anti* to *syn* transformation of a surface-adsorbed polymer backbone toward an unusual thermodynamically stable supramolecular product

Zhi-Xuan Liu[a], Ling Yang[a], Yong-Gang Chen[b], Zhi-Yuan Tian[a] and Zhi-Yong Yang[a]*

a: School of Chemical Science, University of Chinese Academy of Sciences, 19A Yuquanlu, Beijing, 100049, P. R. China. E-mail: yangzhiyong@ucas.ac.cn

b: Dalian University of Technology, No.2 Linggong road, Dalian, 116024, Liaoning province, P. R. China.

Figure S1

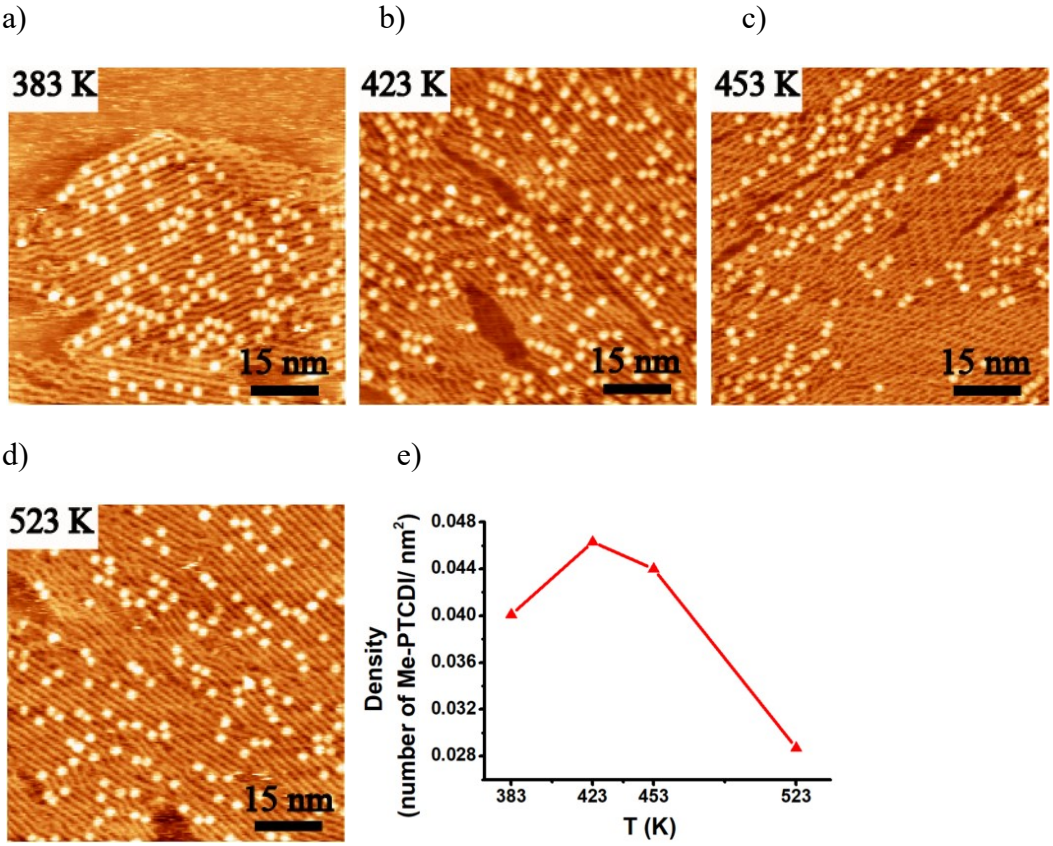

Figure S1 Typical STM images of Me-PTCDI/PffBT4T-2OD samples after annealing 2 h at : (a) 383 K; (b) 423 K; (c) 453 K; (d) 523 K. (e) Alteration of the Me-PTCDI density in Me-PTCDI/PffBT4T-2OD hybrid domains with annealing temperature. Tunneling conditions: (a) V_{tip}=-1.12 V, I_{tip}=0.09 nA; (b) and (c) V_{tip}= -1.12 V, I_{tip}=0.10 nA; (d) V_{tip}= -1.30 V, I_{tip}= 0.06 nA.

Figure S2

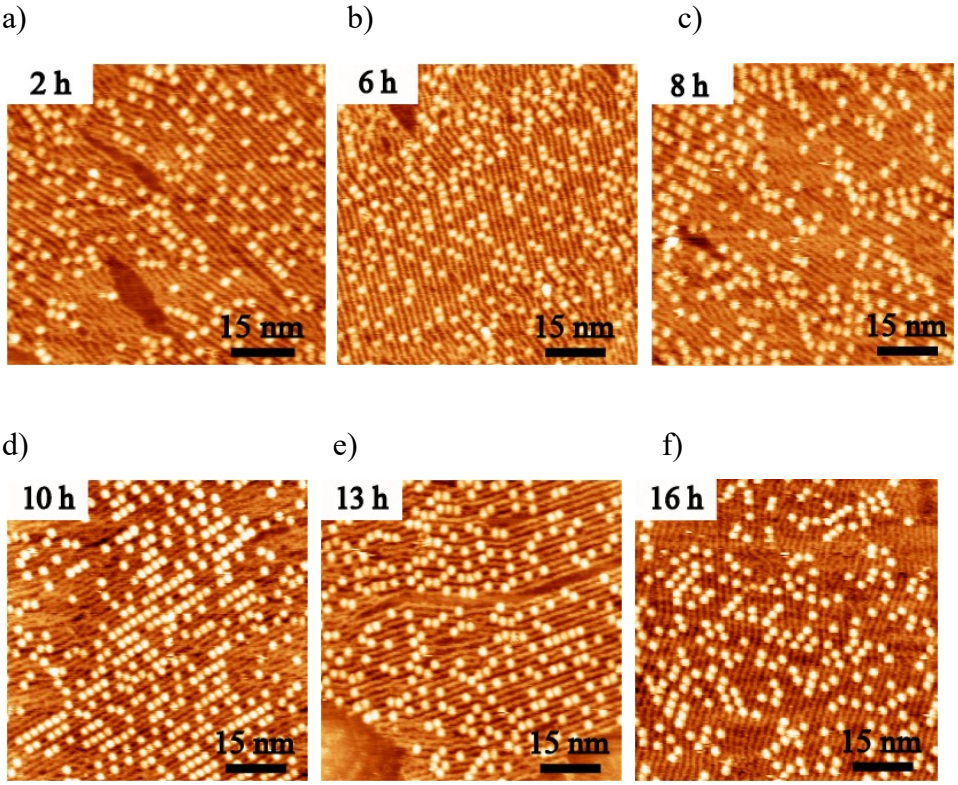

Figure S2 Typical STM images of Me-PTCDI/PffBT4T-2OD annealed at 423 K with: (a) 2 h; (b) 6 h; (c) 8 h; (d) 10 h; (e) 13 h; (f) 16 h. (g) Alteration of the Me-PTCDI density in Me-PTCDI/PffBT4T-2OD hybrid domains with annealing time. Tunneling conditions: (a) V_{tip}=-1.12 V, I_{tip}=0.10 nA; (b) V_{tip}=-1.12 V, I_{tip}=0.12 nA; (c) V_{tip}=-1.12 V, I_{tip}=0.07 nA; (d) V_{tip}=-1.3 V, I_{tip}=0.08 nA; (e) V_{tip}=-1.12 V, I_{tip}=0.09 nA; (f) V_{tip}=-1.3 V, I_{tip}=0.08 nA.

Figure S3

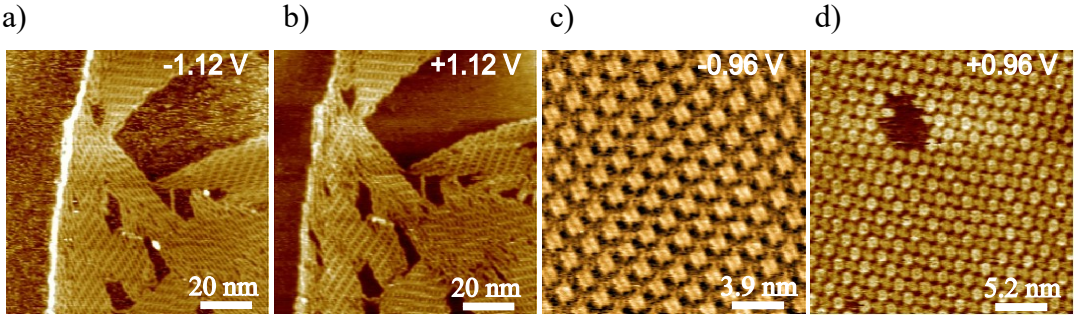

Figure S3 Typical STM images of pure domains of PffBT4T-2OD (a and b, annealed 1.5 h at 363 K) and Me-PTCDI (c and d, annealed 2 h at 453 K). Tunneling conditions: (a) V_{tip}=-1.12 V, I_{tip}=0.19 nA; (b) V_{tip}=1.12 V, I_{tip}=0.19 nA; (c) V_{tip}= -0.96 V, I_{tip}= 0.10 nA; (d) V_{tip}=0.96 V, I_{tip}=0.16 nA.

Figure S4

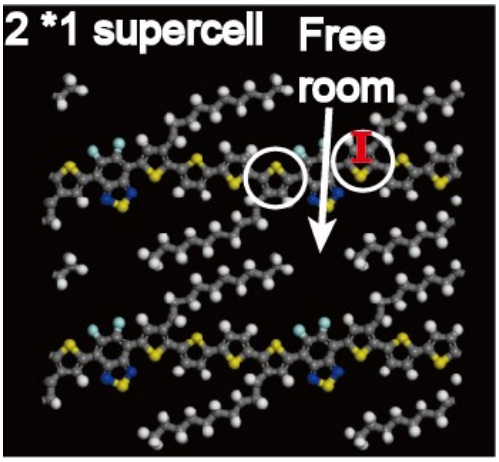

Figure S4 DFT-optimized model of *anti* PffBT4T-2OD stacking. The size of unit cell is a=1.97 nm, b=3.41 nm, c=3.0 nm, $\alpha=\beta=\gamma=90^{o}$. Substrate and lattice lines are set as invisible for clarity. k point mesh set in calculation is 4*2*1. Element color given in Figure 2.

Figure S5

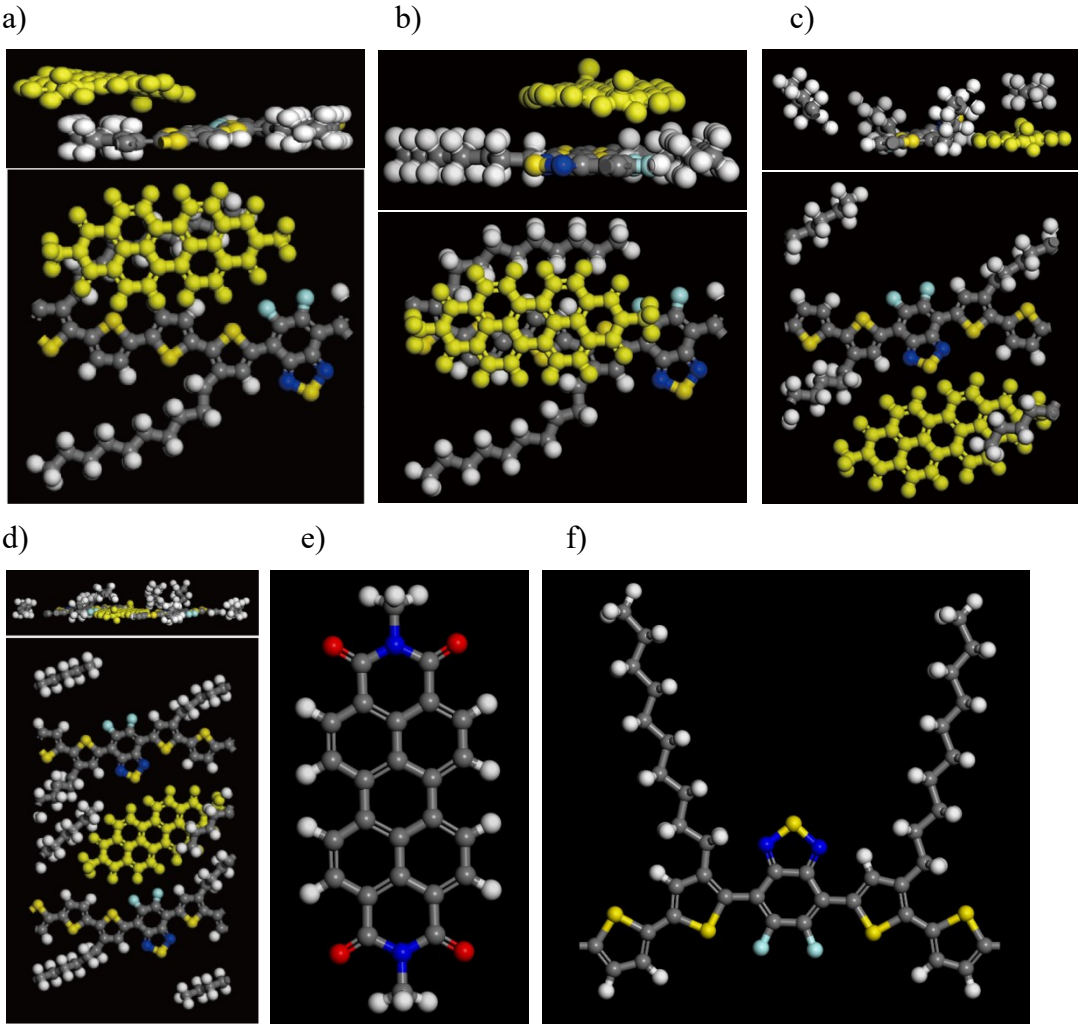

Figure S5 The unit cell of Me-PTCDI on top of PffBT4T-2OD alky chains before (a) and after optimization (b); (c) the optimized unit cell of Me-PTCDI sandwiched between the alky chains of PffBT4T-2OD and substrate; (d) the optimized unit cell of Me-PTCDI sandwiched between the alky chains of PffBT4T-2OD and substrate with the size of unit cell and total number of atoms same to Figure 3c but PffBT4T-2OD is in the *anti* conformation. Isolated Me-PTCDI (e, long axis of Me-PTCDI in *b* direction) and PffBT4T-2OD (f) on substrate. Substrate and lattice lines are set as invisible and Me-PTCDI in (a-d) is colored as yellow for clarity. The size of unit cell is a=1.97 nm, b=1.70 nm, c=3.0 nm, $\alpha=\beta=\gamma=90^{o}$ for (a-c) and a=1.97 nm, b=3.41 nm, c=3.0 nm, $\alpha=\beta=\gamma=90^{o}$ for (d-f). k point mesh set in calculation is 5*5*1 for (a-c) and 4*2*1 for (d-f).

Figure S6

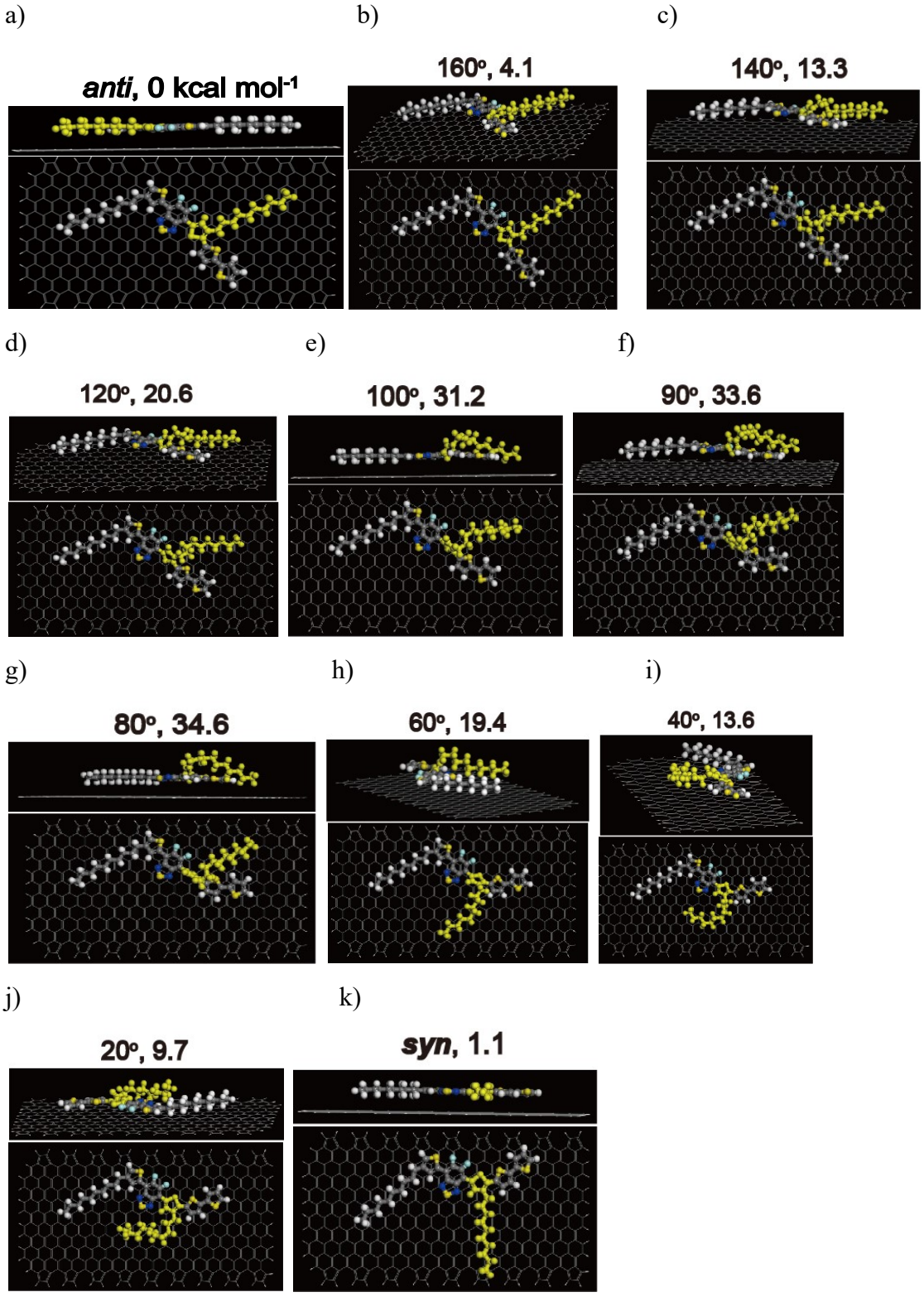

Figure S6 DFT-optimized flipping structures of model PffBT4T-2OD. The dihedral angles in the *anti* and *syn* structures are not fixed during DFT calculations. The energy value is relative to (a) model. The flipping part is colored as yellow for clarity.

Table S1 Binding energy (ΔE*) of the transformation structures of PffBT4T-2OD, Me-PTCDI/PffBT4T-2OD and PffBT4T-2Me shown in Figure S6, S7 and S8, respectively.

Dihedral angles	Binding energy ΔE (kcal mol^{-1})			
	PffBT4T-2OD	Me-PTCDI/PffBT4T-2OD		PffBT4T-2Me
anti	-251.7	*anti* initial	-332.7	-137.9
		anti	-322.5	
160°	-247.7	-318.2		-134.0
140°	-238.5	-317.3		-127.2
120°	-231.2	-312.1		-121.9
100°	-220.5	-307.6		-118.6
90°	-218.2	-305.8		-117.9
80°	-217.2	-305.4		-118.2
60°	-232.4	-320.8		-121.9
40°	-238.1	-		-128.1
20°	-242.1	-		-134.1
syn	-250.6	-		-137.1

*$\Delta E=E_{molecule+substrate}-\Sigma E_{molecule-} - E_{substrate}$

Figure S7

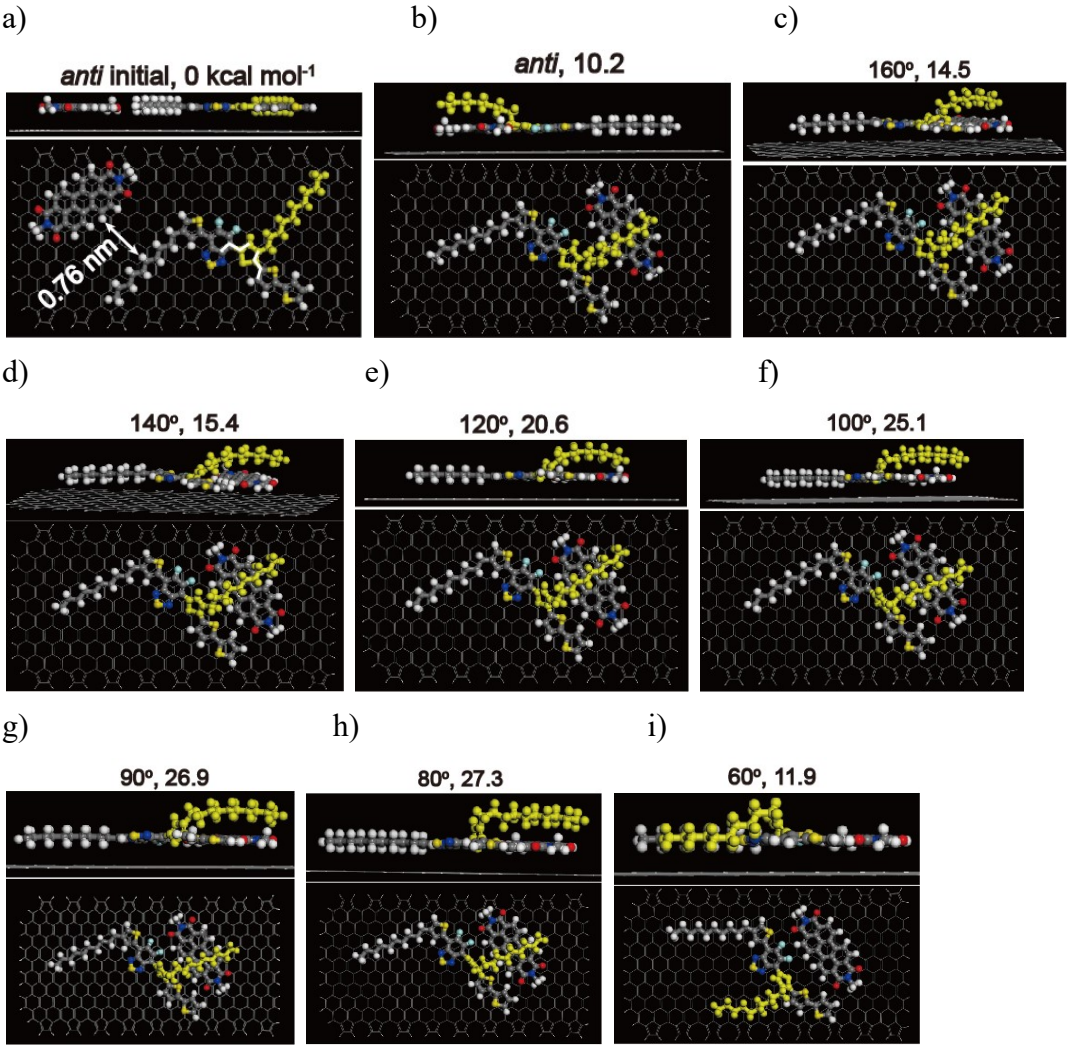

Figure S7 DFT-optimized flipping structures of model Me-PTCDI/PffBT4T-2OD. The dihedral angles in the *anti* initial and *anti* structures are not fixed during DFT calculations. The energy value is relative to (a) model. The flipping part is colored as yellow for clarity.

Figure S8

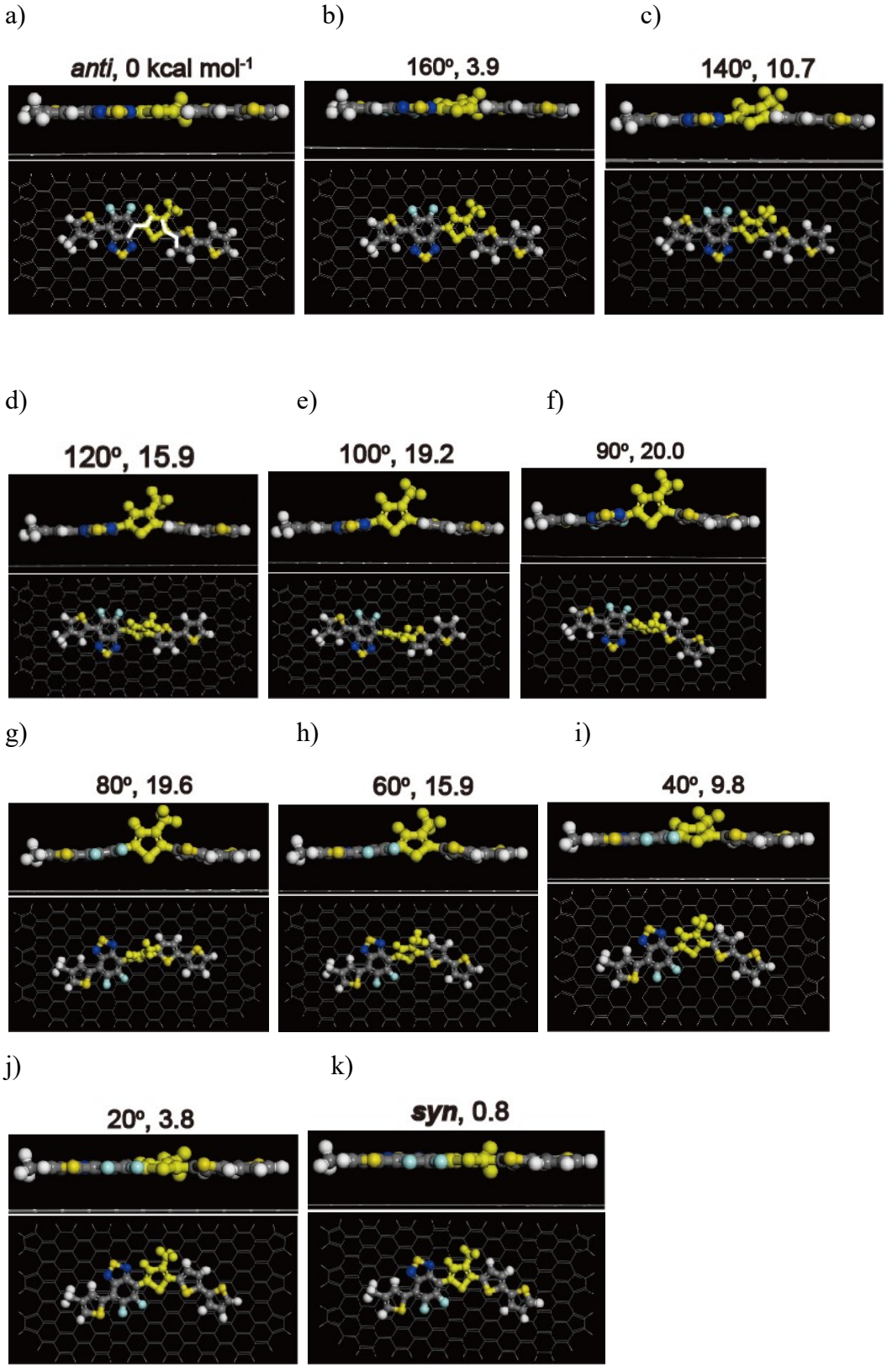

Figure S8 DFT-optimized flipping structures of model PffBT4T-2Me (alkyl chains were changed to methyl groups). The dihedral angles in the *anti* and *syn* structures are

not fixed during DFT calculations. The energy value is relative to (a) model. The flipping part is colored as yellow for clarity.

Figure S9

a) b)

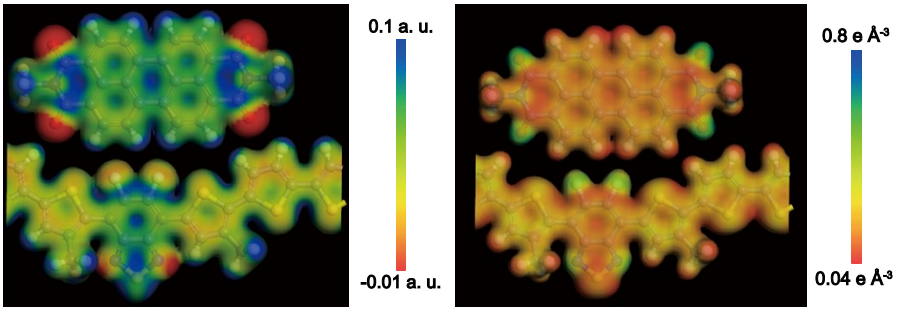

c)

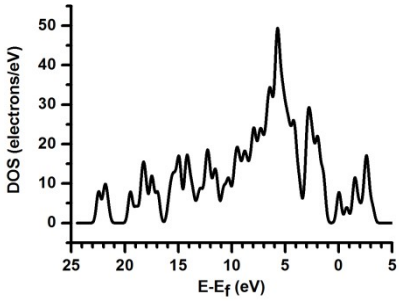

Figure S9 Electrostatic potential (a, projection on the isodensity surface of 0.1 e Å^{-3}) and electron density map (b, projection on the isosurface of 0.1 a.u.) of Me-PTCDI/ PffBT4T-2OD hybrid. (c) Density of state of Me-PTCDI/PffBT4T-2OD hybrid. After optimization on graphene substrate with a periodical box of a=1.97 nm, b=3.41 nm, c=3.0 nm, $\alpha=\beta=\gamma=90^{o}$ and all side chains simplified as methyl, the second-round optimization and property calculations were performed after graphene substrate was removed while keeping the Z position of all atoms fixed. Lattice lines are set as invisible for clarity. k point mesh in DFT calculations is set as 4*1*1.